Ammonia Triborane: Theoretical Study of the Mechanism of Hydrogen Release

ARTICLE *in* THE JOURNAL OF PHYSICAL CHEMISTRY C · JUNE 2007

Impact Factor: 4.77 · DOI: 10.1021/jp0714062

Ammonia Triborane: Theoretical Study of the Mechanism of Hydrogen Release

Vinh Son Nguyen,[†] Myrna H. Matus,[‡] Minh Tho Nguyen,*[,†,‡] and David A. Dixon*[,†]

Department of Chemistry, The University of Alabama, Shelby Hall, Tuscaloosa, Alabama 35487-0336, and Department of Chemistry, University of Leuven, B-3001 Leuven, Belgium

Received: February 19, 2007; In Final Form: April 5, 2007

High-level electronic structure calculations have been used to predict the thermodynamic stability of ammonia triborane $B_3H_7NH_3$ and the molecular mechanism of H_2 elimination from various isomeric forms in the gas phase. Geometries of stationary points were optimized at the second-order perturbation theory MP2 level, and total energies were computed at the coupled-cluster CCSD(T) theory with the aug-cc-pVnZ (n = D, T, Q) basis sets and extrapolated to the complete basis set limit. Heats of formation for the structures considered in the gas phase were evaluated at both 0 and 298 K. The lowest-energy process for H_2 release from the most stable isomer of $B_3H_7NH_3$ is a 1,3-elimination characterized by an energy barrier of 28.9 kcal/mol. Although the barrier height for H_2 release from $B_3H_7NH_3$ is slightly smaller than the B−N bond cleavage energy of 30.7 kcal/mol yielding $B_3H_7 + NH_3$, the calculated rate coefficients predict that bond cleavage is faster than H_2 release by 3 orders of magnitude at 298 K and 1 atm. We predict the heat of formation for the most stable isomer of B_3H_7 to be ΔH_f (0 K) = 37.1 ± 0.8 kcal/mol and ΔH_f (298 K) = 32.5 ± 0.8 kcal/mol, and for the most stable isomer of $B_3H_7NH_3$ to be ΔH_f (0 K) = 0.4 ± 1.0 kcal/mol and ΔH_f (298 K) = −7.1 ± 1.0 kcal/mol.

Introduction

Hydrogen-based fuel cells are currently being considered as a power source for many applications, including on-board transportation systems.[1] Critical issues for the use of hydrogen as a fuel include the development of efficient and safe H_2 storage materials. Amine boranes and derivatives have been proposed as potential hydrogen sources.[2−5] Ab initio electronic structure theory calculations of reaction thermodynamic parameters, both in the gas phase and in the solid state,[6,7] showed that borane amine (BH_3NH_3) and the corresponding salts ($[BH_4^-][NH_4^+]$) can indeed serve as good hydrogen storage systems that release H_2 in slightly exothermic processes.[6] Hydrogen release from amine borane has been predicted to be greatly facilitated by the presence of an additional borane molecule (BH_3), which can act as a Lewis acid bifunctional catalyst.[8]

Yoon and Sneddon[9] recently reported that the long-known[10−12] ammonia triborane has properties which also make it a promising candidate for amine borane-based chemical hydrogen storage, and presented an efficient, convenient, and safe method for its preparation. They report that oxidative hydrolysis of $B_3H_7NH_3$ in aqueous solution leads to the release of up to 8 equiv of H_2, upon addition of either acids or metal catalysts (such as $RhCl_3$).

As part of our efforts in predicting the energetic properties of H_2 storage materials using high-level molecular orbital theory, we have studied the thermodynamic and kinetic properties of ammonia triborane.

Computational Methods

The calculations were performed by using the *Gaussian03*[13] and *MOLPRO*[14] suites of programs. The geometry parameters were initially optimized using second-order perturbation theory (MP2)[15] in conjunction with the correlation consistent aug-cc-pVDZ basis set[16] (denoted hereafter as aV*n*Z, with n = D, T, and Q). The character of each stationary point was determined to be an equilibrium structure or a first-order saddle point, by calculations of harmonic vibrational frequencies at the same level. To ascertain the identity of the transition state structures (TS), forward and reverse intrinsic reaction coordinate (IRC)[17] calculations were carried out at the MP2/aVDZ level with the default step size of 0.1 amu$^{1/2}$-bohr. Geometry parameters of relevant structures were then reoptimized using the MP2 method with the larger aVTZ basis set. The latter optimized geometries were subsequently utilized for single-point electronic energies using coupled-cluster CCSD(T) theory.[18] In all MP2 and CC calculations, the core orbitals were kept frozen. The ZPEs were evaluated by using MP2/aug-cc-pVDZ vibrational frequencies and scaled by factors of 0.9787 for boron hydrides (B_nH_m) and 0.9876 for ammonia borane derivatives. The scaling factors were derived on the basis of previous evaluations of ZPEs for related compounds, B_2H_6[19,20] and BH_3NH_3.[6]

The potential energy surface was initially mapped at the CCSD(T)/aVTZ calculations with appropriate ZPE corrections. The final critical energies were obtained by extrapolating CCSD(T)/VnZ calculations to the complete basis set (CBS) limit by using the following expression:[21]

$$E(x) = A_{CBS} + B \exp[-(n-1)] + C \exp[-(n-1)^2] \quad (1)$$

with n = 2, 3, and 4 for the aV*n*Z, n = D, T, and Q basis sets, respectively.

The total atomization energy (ΣD_0 or TAE) of a compound is given by the expression

$$\Sigma D_0 = \Delta E_{elec}(CBS) - \Delta E_{ZPE} + \Delta E_{CV} + \Delta E_{SR} + \Delta E_{SO} \quad (2)$$

* E-mail: dadixon@bama.ua.edu.
† University of Leuven.
‡ The University of Alabama.

10.1021/jp0714062 CCC: $37.00
Published on Web 06/05/2007

TABLE 1: Components for Atomization Energies in kcal/mol

molecule	ΔE_{CBS} [a]	ΔE_{ZPE}	ΔE_{CV} [b]	ΔE_{SR} [c]	ΔE_{SO} [d]	ΣD_0(0 K)[e]
tb1	771.88	46.12[f]	3.82	-0.23	-0.09	729.25
tb2	776.00	46.70[f]	3.91	-0.24	-0.09	732.88
tb3	766.78	46.12[f]	3.65	-0.23	-0.09	723.99
atb3-c	1074.06	70.94[g]	4.26	-0.53	-0.09	1006.75
atb3-c1	1095.12	72.86[g]	4.52	-0.54	-0.09	1026.15
atb3-t	1074.57	70.94[g]	4.25	-0.53	-0.09	1007.26
atb3-t1	1093.28	72.71[g]	4.52	-0.54	-0.09	1024.45
atb1	1105.89	72.95[g]	4.71	-0.55	-0.09	1037.00
atb1-p1	983.40	59.29[g]	4.60	-0.54	-0.09	928.08
atb1-ts1	1073.38	69.30[g]	4.63	-0.55	-0.09	1008.08
atb1-ts2	1055.36	68.87[g]	4.66	-0.56	-0.09	990.49

[a] Extrapolated by using eq 1 at the CCSD(T)/aV*n*Z level with n = D, T, and Q. [b] Core/valence corrections were obtained by CCSD(T)/cc-pwCVTZ. [c] Scalar relativistic corrections based on CISD/aug-cc-pVTZ calculations. [d] Values obtained from ref 24. [e] Total dissociation energy: $\Sigma D_0 = \Delta E_{elec}(CBS) - \Delta E_{ZPE} + \Delta E_{CV} + \Delta E_{SR} + \Delta E_{SO}$. [f] A scale factor of 0.9787, obtained from the MP2/aug-cc-pVDZ ZPE and experimental values (see ref 20) for B_2H_6. [g] A scale factor of 0.9876, obtained from the MP2/aug-cc-pVDZ ZPE and that obtained in ref 6 for BH_3NH_3.

TABLE 2: Gas-Phase Heats of Formation at 0 and 298 K (kcal/mol) and Entropies at 298 K (cal/mol·K)

molecule	ΔH_f (0 K) CCSD(T)	ΔH_f (298 K) CCSD(T)[a]	S (298 K)[b]
tb1	40.8	36.3	64.70[c]
tb2	37.1	32.5	64.00[c]
tb3	46.0	41.9	67.60[c]
atb3-c	30.7	23.8	78.80[d]
atb3-c1	11.3	4.0	76.20[d]
atb3-t	30.2	23.5	80.70[d]
atb3-t1	13.0	5.8	78.40[d]
atb1	0.4	-7.1	73.63,[c] 74.10[d]
atb1-p1	6.1	0.3	71.86[c]
atb1-ts1	29.4	21.5	70.89[c]
atb1-ts2	46.9	39.3	73.00[d]
NH_3	−9.6,[e] −9.30 ± 0.10[f]	−11.3,[e] −10.97 ± 0.10[f]	45.96,[c] 46.07[f]

[a] The theoretical values at 298 K obtained by the same procedure as in ref 30. [b] $S(H_2)$ = 31.13 cal/mol-K from ref 28. [c] MP2/aug-cc-pVTZ values. [d] MP2/aug-cc-pVDZ values. [e] ref 6. [f] ref 28.

Core-valence corrections, ΔE_{CV}, were obtained at the CCSD(T)/cc-pwCVTZ level.[22] Scalar relativistic corrections, ΔE_{SR}, were included at the CI-SD (configuration interaction singles and doubles) level of theory using the aug-cc-pVTZ basis set. ΔE_{SR} is taken as the sum of the mass−velocity and 1-electron Darwin (MVD) terms in the Breit−Pauli Hamiltonian.[23] For the total atomization energies, no spin−orbit correction is needed for N in the ^4S state, but a correction of 0.03 kcal/mol was included for B, taken from the excitation energies of Moore.[24] The single-point electronic energies for the atoms were calculated using the restricted coupled-cluster R/UCCSD(T) formalism. In this approach, a restricted open-shell Hartree−Fock (ROHF) calculation was initially performed, and the spin constraint was relaxed in the coupled cluster calculation.[25−27]

By combining our computed ΣD_0 (total atomization energies) values with the known heats of formation at 0 K for the elements (ΔH_f°(N) = 112.53 ± 0.02 kcal mol^{-1}, ΔH_f°(B) = 136.2 ± 0.2 kcal mol^{-1}, and ΔH_f°(H) = 51.63 kcal mol^{-1}),[28,29] we can derive ΔH_f° values for the molecules under study in the gas phase. To obtain the heats of formation at 298 K, we followed the procedure by Curtiss et al.[30] All values shown in the figures and discussed in the text were obtained from the atomization energies (CCSD(T)/CBS + corrections level) to two decimal places unless otherwise noted.

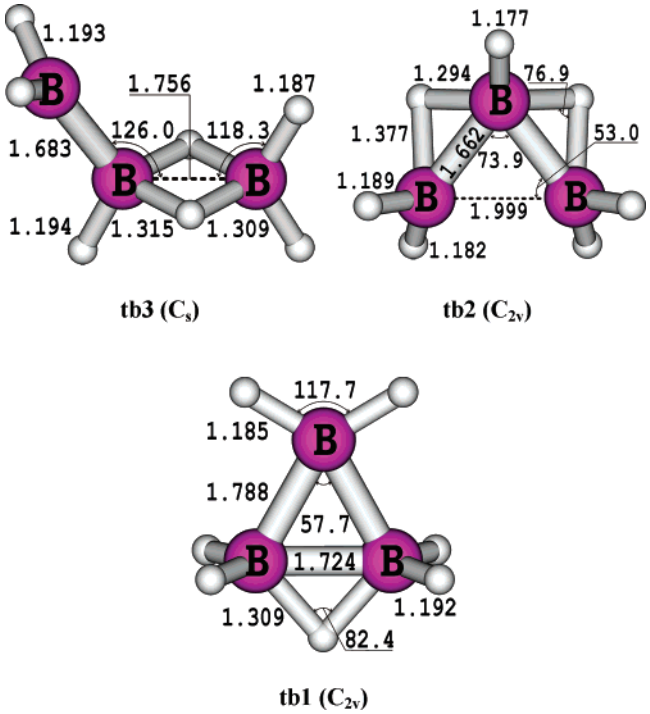

Figure 1. Selected MP2/aVTZ geometrical parameters of three triborane isomers. Bond distances are given in angstroms and bond angles in degree.

TABLE 3: Relative CCSD(T) Energies of the Three B_3H_7 and the Five $B_3H_7NH_3$ Isomers[a]

	basis set			
isomer	aVDZ	aVTZ	aVQZ	CBS[b]
tb3	6.72	8.16	8.48	8.64
tb2	0.0	0.0	0.0	0.0
tb1	2.63	3.32	3.47	3.54
atb3-c	27.50	29.27	29.65	29.85
atb3-t	27.02	28.76	29.14	29.33
atb3-c1	9.84	10.50	10.62	10.68
atb3-t1	11.64	12.22	12.32	12.37
atb1	0.0	0.0	0.0	0.0

[a] Values in kcal/mol based on MP2/aVTZ geometries (cf. Figures 1 and 2) and with ZPE corrections. [b] From extrapolated energies using eq 1.

Results and Discussion

The components for the total atomization energies are given in Table 1 and the predicted heats of formation at 0 and 298 K are given in Table 2. Relative energies calculated using the CCSD(T) method as a function of basis set are compared in Table 3. The relative energies quoted in the following sections refer to, unless otherwise noted, those derived from the calculated heats of formation at 0 K. The aVDZ results are semiquantitative within ~2 kcal/mol, and those obtained with the aVTZ basis set differ by 0.5 kcal/mol or less with respect to the CBS values.

Relative Energies of B_3H_7 Isomeric Forms. We first considered the triborane B_3H_7. Early theoretical studies with geometry optimization at the Hartree−Fock level with small basis sets[31] identified five different structures for B_3H_7. More recent theoretical studies[32,33] using the G3 and CCSD(T) methods considered only one[32] or two[33] low-lying isomers. Our MP2 geometry optimizations and vibrational analyses located the three equilibrium structures **tb1**, **tb2**, and **tb3** shown in Figure 1 where we use the convention that **tb** is the triborane

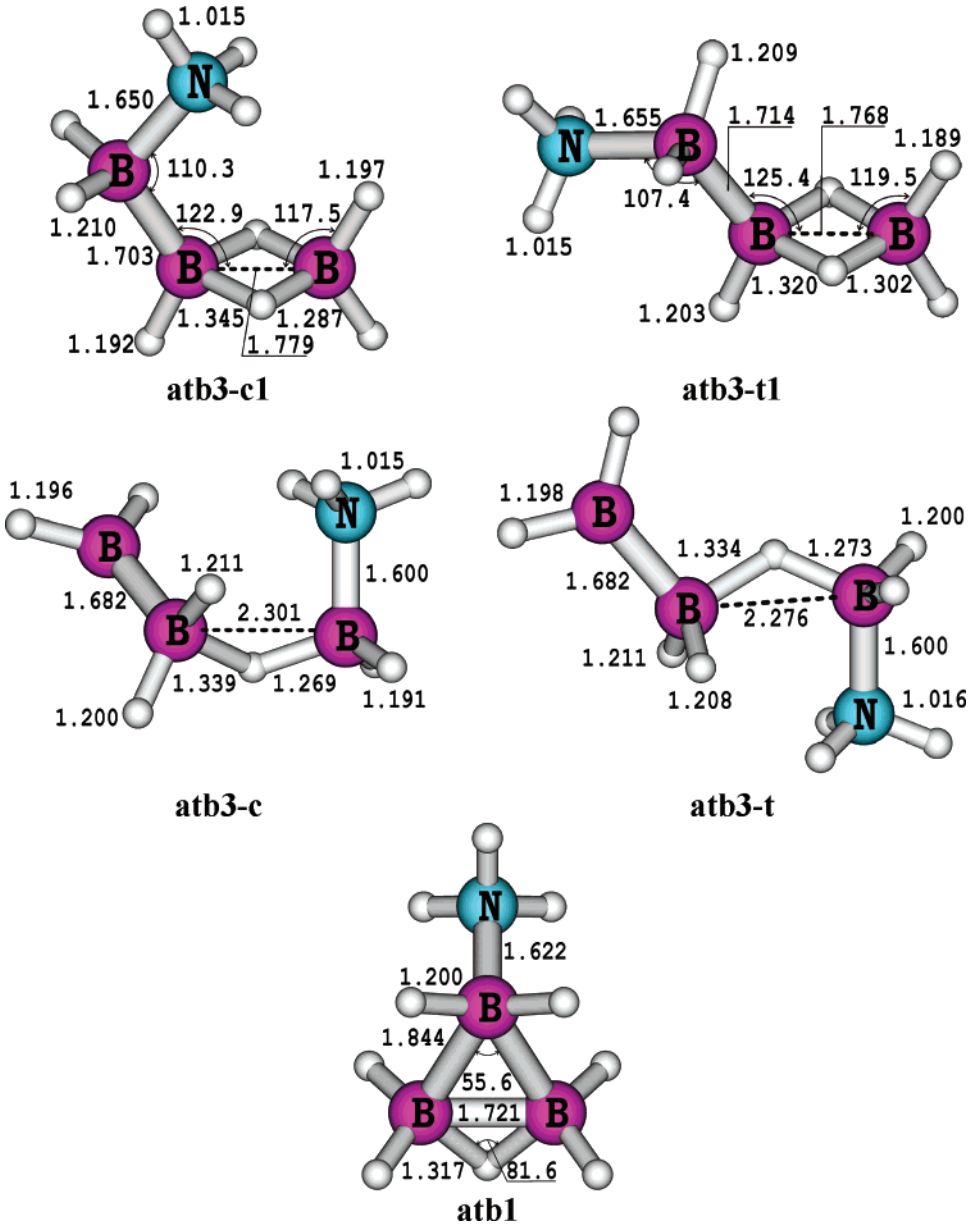

Figure 2. Selected MP2/aVTZ geometrical parameters of the ammonia triborane $B_3H_7NH_3$ isomers. Bond distances are given in angstroms and bond angles in degree.

B_3H_7. Other possible structures were not found to be local energy minima. The calculated relative energies (Table 3) are well-converged at the CCSD(T)/aVTZ and CCSD(T)/aVQZ levels which differ by only 0.5 and 0.1 kcal/mol from the CCSD-(T)/CBS values, respectively.

In agreement with the earlier studies,[32,33] the dibridge form **tb2** with two three-center two-electron B−H−B bonds is found to be the most stable isomer. Following the normal conventions for B_xH_y clusters, there is no formal bond between the two nonbridge boron atoms in **tb2**. This is consistent with the fact that the B−B bond distance is quite long at 1.999 Å. The triangular monobridge form **tb1**, with a single three-center two-electron B−H−B bond, which was reported in the earlier theoretical study by Lipscomb and co-workers[31] but not considered in the most recent study by Tian,[33] is only 3.7 kcal/mol higher in energy than **tb2**. **tb1** can be considered to be a diborane molecule with a bridging H replaced by a bridging BH_2. The bridging BH_2 is essentially in the B−H−B plane. The open structure **tb3**, which was considered by Tian,[33] is predicted to be 8.9 and 5.2 kcal/mol above **tb2** and **tb1**, respectively. Our value of 8.9 kcal/mol is slightly larger than the value of 8.3 kcal/mol obtained from CCSD(T) calculations with the smaller 6-311G(d,p) basis set.[33] **tb3** is best described as a diborane where a terminal H is replaced by a BH_2 group. The terminal BH_2 group is oriented so that its empty p orbital is in the plane perpendicular to the B−H−B bonds. The most stable structure is the one that is not based on substituting BH_2 for H in diborane. Replacing the bridging H with BH_2 to form **tb1** is lower in energy than replacing a terminal H in diborane to form **tb3**. As discussed below, **tb1** plays a key role in the condensation with an ammonia molecule. For the most stable form (**tb2**), we predict heats of formation of $\Delta H_f(0\ K) = 37.1 \pm 1.0$ kcal/mol and $\Delta H_f(298\ K) = 32.5 \pm 1.0$ kcal/mol. These values differ in a significant way (~7 kcal/mol) from earlier G3 values also obtained by atomization energies: $\Delta H_f(0\ K) = 30.0$ kcal/mol and $\Delta H_f(298\ K) = 25.6$ kcal/mol.[32] This difference is, in addition to the theoretical method, due mostly to the use of the old heat of formation for the boron atom used by Cheng et al.,[32] $\Delta H_f(0\ K) = 133.27$ kcal/mol and $\Delta H_f(298\ K) = 134.49$ kcal/mol, which has been shown to be incorrect.

Structure of $B_3H_7NH_3$ Isomers. The interaction of ammonia with B_3H_7 can lead to several Lewis acid−base condensation $B_3H_7NH_3$ molecules. The NH_3 acts as a Lewis base (nucleophilic agent) interacting with the Lewis acid electron-deficient borane. It has previously been shown that the geometries of the resulting adducts differ significantly from those of the boranes.[34] Figure 2 displays the five ammonia triborane adducts with a selection of MP2/aVTZ geometry parameters. In general, each isomer is designated by the letter **atb*X*-*y***, in which **atb*X***, with ***X*** = **1** and **3**, stands for an ammonia triborane resulting from **tbX**; ***y*** = **c**, **c1**, **t**, and **t1** refer to cis and trans configurations, respectively. The relative energies are reported in Table 3.

Adducts will be more readily formed starting from boranes with a vacancy on boron.[34] Thus, NH_3 complexation to **tb1** and **tb3** should yield lower-energy adducts than that formed from the more stable **tb2**. Indeed, in spite of extensive searching, no adduct between NH_3 and **tb2** could be located. All geometry optimizations invariably converged to **atb1**, which is the natural adduct of **tb1** and ammonia. In this case, the adduct is formed by stabilizing the bridging BH_2 group by interacting with the vacant p orbital on the bridging BH_2. The B−N bond distance of 1.622 Å (Figure 2) is shorter than to that of 1.659 Å in BH_3-NH_3 derived at the same level.[6] Nordman and Reimann[10] determined the crystal structure of ammonia triborane, but it was not possible to provide a conclusive structure on the basis of the experimental electron density distribution. These authors[10b] suggested that the boron triangle in $B_3H_7NH_3$ is held together by two B−H−B bridge bonds and one B−B electron pair (as in **tb2**), but did not rule out the alternative description in terms of one hydrogen bridge and a central three-center bond. Their alternative form is confirmed by our calculations to be the most stable structure (**atb1**). The crystal structure was found to be significantly distorted without point group symmetry having the following bond distances: B−N, 1.581 ± 0.003 Å; B−B (opposite to NH_3), 1.744 ± 0.005 Å; B−B, 1.820 ± 0.006 Å; and B−B, 1.803 ± 0.006 Å. Our MP2 values differ from these experimental ones by about 0.02 Å (Figure 2).

Condensation of NH_3 to the open form **tb3** results in a larger number of adducts, due to the relative orientation of the incoming NH_3 group with respect to the other moiety. **atb3-c1** and **atb3-t1** correspond to cis and trans conformations of the adduct derived from complexation at the terminal BH_2 group. This corresponds to the NH_3 interacting with the vacant orbital on the terminal BH_2 group just as in NH_3BH_3 except that one of the H's on the BH_3 has been replaced by a B_2H_5 fragment. The B−N distances of 1.650−1.655 Å in both conformers are similar to the value of 1.659 Å predicted for BH_3NH_3. The B−B distances of 1.703−1.714 Å are stretched relative to that of 1.683 Å in **tb3**, due to the presence of the new N−B bond.

atb3-c and **atb3-t** are formed by addition of NH_3 to the BH_2 group in the diborane fragment, which leads to another pair of cis and trans conformations. Upon complexation, one of the bridge B−H−B bond of **tb3** breaks, leading to a complex of BH_3NH_3 with BH_2BH_2 where a B−H bond from BH_3NH_3 interacts with the vacant p orbital on the BH_2 bonded to the other BH_2. This condensation is similar to that between BH_3-NH_3 and BH_3 discussed recently by us.[8] Replacement of an H atom of BH_3 by BH_2 (giving BH_2BH_2) does not induce significant geometric changes. The B−N bond distance of 1.60 Å in both adducts **atb2-c1** and **atb3-t1** is nearly identical with that in the $BH_3NH_3BH_3$ complex (MP2/aVTZ geometry). The B−H−B bond distances in these structures are also similar.[8]

The results recorded in Table 2 clearly show that the adduct **atb1** is by far the most stable form with **atb1** thermodynamically

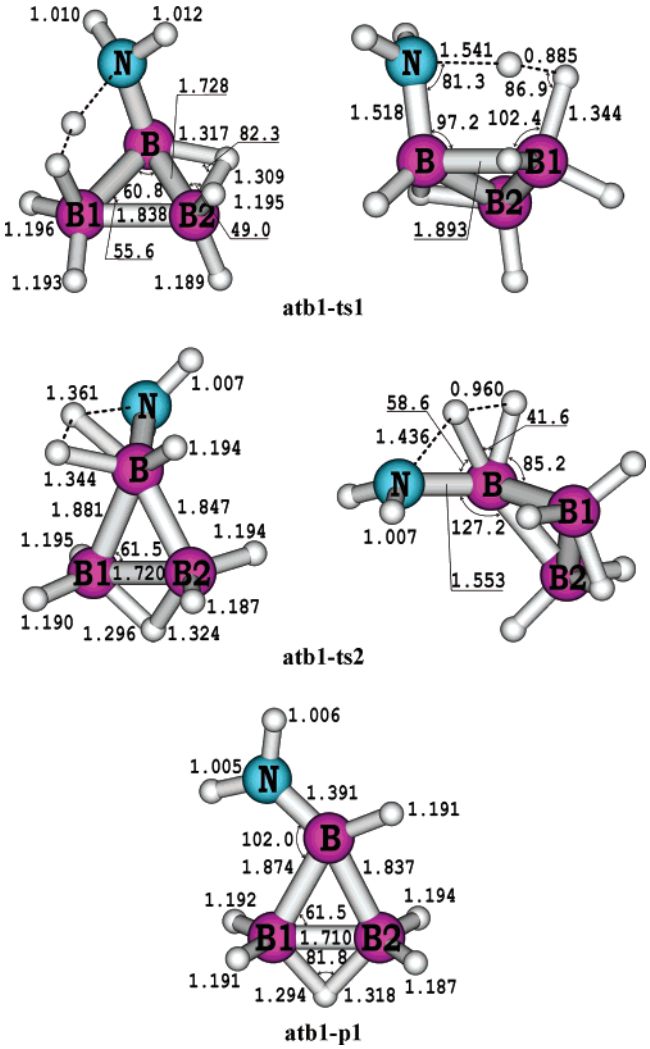

Figure 3. Selected MP2/aVTZ geometrical parameters of two transition state structures and product from the H_2 elimination of **atb1**. Bond distances are given in angstroms and bond angles in degree. For **atb1-ts1** and **atb1-ts2**, two different views are presented.

more stable by 10.9 kcal/mol than **atb3-c1**. Of the **c1**/**t1** pair, **atb3-c1** is about 1.7 kcal/mol more stable than **atb3-t1.** Of the **c**/**t** conformers, **atb3-t** is slightly (0.5 kcal/mol) more stable than **atb3-c**. **atb3-t** is substantially higher in energy, about 29.8 kcal/mol above **atb1** and 18.9 kcal/mol above **atb3-c1**. With respect to the B−N bond scission, **atb3-c1** is 25.1 kcal/mol lower in energy than the separated fragments **tb3** + NH_3, which is slightly smaller than the value of 25.9 kcal/mol for BH_3NH_3 with respect to BH_3 + NH_3 at the same level of theory.[8]

Westrum and Levitin measured the heat capacity of the solid and the heat of sublimation of **atb1**[12] to be 17.1 ± 0.1 kcal/mol, and they estimated a gas-phase entropy *S* to be 68.8 cal/mol−K. By using the experimental value for the heat of sublimation, we can estimate that the heat of formation of solid $B_3H_7NH_3$ is −24.2 kcal/mol at 298 K. Our calculated entropy for **atb1** is *S* = 73.6 cal/mol−K. The estimated entropy is in qualitative agreement with our calculated value.

The bond energy of adduct **atb1** for B−N bond cleavage is 32.1 kcal/mol at 298 K and 30.7 kcal/mol at 0 K

$$NH_3B_3H_7\ (\mathbf{atb1}) \rightarrow NH_3 + B_3H_7\ (\mathbf{tb1}) \qquad (3)$$

Previous MP2/6-31G(d) calculations predicted a larger value of 42.9 kcal/mol for this quantity.[34] The B−N σ dative bond

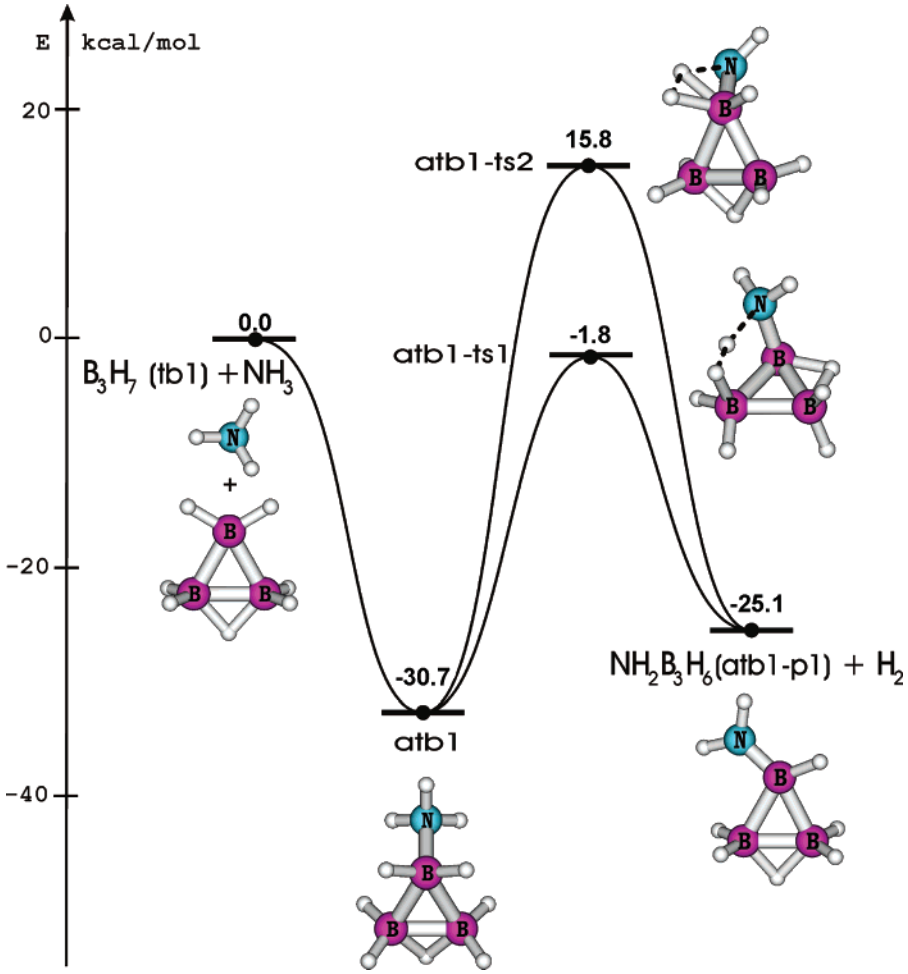

Figure 4. Schematic energy profiles illustrating two different reaction pathways for H_2 release from **atb1**. Relative energies, in kcal/mol, were obtained from the atomization energies (CCSD(T)/CBS + corrections) at 0 K.

energy in **atb1** is stronger than the B−N bond in BH_3NH_3 (25.9 kcal/mol).[6] The corresponding B−N bond energies for the terminal adducts are lower than the value in BH_3NH_3, amounting to 25.1 and 23.4 kcal/mol for the cis **atb3-c1** and trans **atb3-t1** isomers, respectively. The B−N adducts formed by addition to the boron in the diborane fragment have very low bond energies of 6.2 kcal/mol in **atb3-t** and 5.7 kcal/mol **atb3-c**, comparable to the value of 5.1 kcal/mol in $B_2H_6NH_3$ (the heat of formation at 0 K of the latter complex is −1.0 kcal/mol derived from a total atomization energy of 850.56 kcal/mol reported in ref 8; the heat of formation of diborane is 13.7 ± 1.4 kcal/mol at 0 K).[35]

In comparison to BH_3NH_3, $B_2H_6NH_3$ is markedly less stable with respect to the B−N bond scission. Formation of an adduct between NH_3 and B_2H_6 requires breaking one of the two B−H−B bonds such as in **atb3-c**. The absence of a second B−H−B bond in the adduct destabilizes it with respect to the separated reactants. In contrast, BH_3NH_3 and $B_3H_7NH_3$ have comparable σ dative B−N bond energies. The interaction of B_3H_7 with a three-membered BBB ring (**tb1**) with NH_3 to form $B_3H_7NH_3$ leads to a stabilization of the adduct **atb1**, which is larger than that in BH_3NH_3. For the most stable isomer of B_3H_7-NH_3 (**atb1**), we predict the heat of formation to be $\Delta H_f(0\ K) = 0.4 \pm 1.0$ kcal/mol and $\Delta H_f(298\ K) = -7.1 \pm 1.0$ kcal/mol.

Reaction Pathways for H_2 Release from $B_3H_7NH_3$ Starting from atb1. We first consider the molecular mechanism for hydrogen elimination from the most stable ammonia triborane **atb1**. Figure 3 displays the two transition structures and the product associated with this process. The letters **ts** and **p** stand for a transition state structure and product, respectively. Calculated energies are summarized in Tables 1 and 2 and in Figure 4, which includes the energy profiles schematically illustrating the pathways under consideration. The connections between two different **ts**'s and the same equilibrium structures shown in Figure 4 were confirmed by IRC calculations. The optimized geometry of the product is given in Figure S-1 of the Supporting Information.

In general, the departing H_2 molecule is composed of one H-atom from the NH_3 fragment and another from the B_3H_7 fragment. The main difference between the two transition states is the position of the H(B) atom. In **atb1-ts1**, the migrating H is coming from atom B1 of the B_2H_5 moiety, situated opposite to ammonia with respect to the central boron B. This process can be described as a 1,3-H_2-elimination. A remarkable feature of this transition state is that, once the H(B1) atom of **atb1** is moving toward the H(N) atom to form the departing H_2, the bridging H-atom migrates in a similar direction, breaking the B1−H−B2 bond and forming a new B1−H bond. A hydrogen bonded to the central boron B shifts in a different direction to generate a new bridge B−H−B2 bond. As a consequence, the two-electron-three-center bond in **atb1-ts1** is now situated adjacent to the ammonia group, in contrast to that in the equilibrium structure **atb1**. As illustrated in Figure 3, the B−N−H−H−B framework of **atb1-ts1,** in which the H_2 formation actually occurs, constitutes a nearly planar five-membered ring with a BB1HH dihedral angle of only 5°. The B1−H distance of 1.344 Å is longer than the normal B−H bond distance (about 1.19 Å), whereas the N−H bond of 1.541 Å is significantly

stretched as compared with a normal N−H bond distance (around 1.01 Å). The B−B1 bond in **atb1-ts1** is elongated by ∼0.05 to ∼0.1 Å to 1.893 Å as compared to 1.788 Å in **tb1** and 1.844 Å in **atb1**. In contrast, the B−N distance of 1.518 Å shortens by ∼0.1 Å relative to that of 1.622 Å in **atb1**. The H−H distance of 0.885 Å in **atb1-ts1** is relatively short, consistent with the hydrogen molecule being mostly formed. The N−H−H−B1 framework formally corresponds to a type of dihydrogen bond with a charge distribution $N^{\delta+}-H^{\delta-}-H^{\delta+}-B^{\delta+}$, which stabilizes the **ts** and facilitates the molecular hydrogen formation. This type of bonding is consistent with what is found in the dimer of BH_3NH_3 and in the solid state.[36,37]

In the second pathway (**atb1-ts2**), the H(B) atom of the departing H_2 originates from the central boron atom of **atb1** (denoted as B in Figure 3). It thus resembles the transition state for H_2 release from BH_3NH_3,[8] where the departing H_2 in the corresponding transition state is centered on the boron atom. The B−H distance of 1.344 Å of **atb1-ts2** is similar to that for the transition state for elimination in BH_3NH_3, and the N−H distance of 1.436 Å and H−H distance of 0.96 Å (0.99 Å in the transition state of BH_3NH_3) are slightly shorter. By using the H−H distance in the transition state as a crude index, **atb1-ts2** is an earlier transition state than is **atb1-ts1**. The B−H−H−N framework of the former is more bent than that of the latter (within a four-membered ring). The process through **atb1-ts2** can be described as a 1,2-H_2-elimination, similar to the pathway found in ammonia borane BH_3NH_3,[8] from which a nonmigrating H(B) atom is replaced by a B_2H_5 group to yield **atb1-ts2**.

1,3-H_2-elimination is predicted to have a substantially lower barrier as compared to 1,2-H_2-elimination. At the CCSD(T)/CBS + ZPE level, the energy barrier for H_2 release from ammonia triborane **atb1** is 28.9 kcal/mol via **atb1-ts1**, but it is 46.5 kcal/mol via **atb1-ts2**. Thus, the energy barrier for 1,3-H_2-elimination is 1.8 kcal/mol below the dissociation energy to form $NH_3 + B_3H_7$, but 1,2-H_2-elimination occurs above this dissociation limit. Both reaction pathways lead to the same product **atb1-p1**, which is an amino-substituted triborane (Figure 3). The forward process **atb1** → **atb1-p1** + H_2 is calculated to be endothermic by 5.6 kcal/mol at the CCSD(T)/CBS + corrections level and 5.7 kcal/mol from the heats of formation at 0 K.

Figure 5 displays the reaction pathways for H_2 release from the parent homologues BH_3NH_3 and $B_2H_6NH_3$ with relative energies obtained at the CCSD(T)/aVTZ + ZPE level of calculation. In each system, the reference point is given to the energy of the separated fragments $B_xH_y + NH_3$. Some important energetic differences are now given. As stated above, B_3H_7-NH_3 **atb1** is more stable than BH_3NH_3 and $B_2H_6NH_3$ with respect to B−N bond cleavage. H_2 release is endothermic by 5.6 kcal/mol from $B_3H_7NH_3$ **atb1** and 10.2 kcal/mol from B_2H_6-NH_3, whereas it is exothermic by a similar amount of 6.3 kcal/mol (CCSD(T)/aVTZ + ZPE) from BH_3NH_3 (Figure 5A). The energy barrier for 1,2-H_2-elimination of 46.5 kcal/mol via **atb1-ts2** is substantially larger than that of 36.8 kcal/mol at the CCSD(T)/aVTZ + ZPE level (36.4 kcal/mol at the CCSD(T)/CBS + corrections level) calculated for the same process in BH_3NH_3.[8] Thus, the substitution of B_2H_5 for H leads to an increase in the barrier height. The $B_2H_6 + NH_3$ channel proceeds through the same adduct as the $BH_3NH_3 + BH_3$ channel would. The condensation of ammonia with diborane (in the reverse, B−N bond breaking in the adduct) is associated with transition state **ts1** in Figure 5B. This corresponds to a breaking/forming of the strong bridge B−H−B bond. The structural and energetic

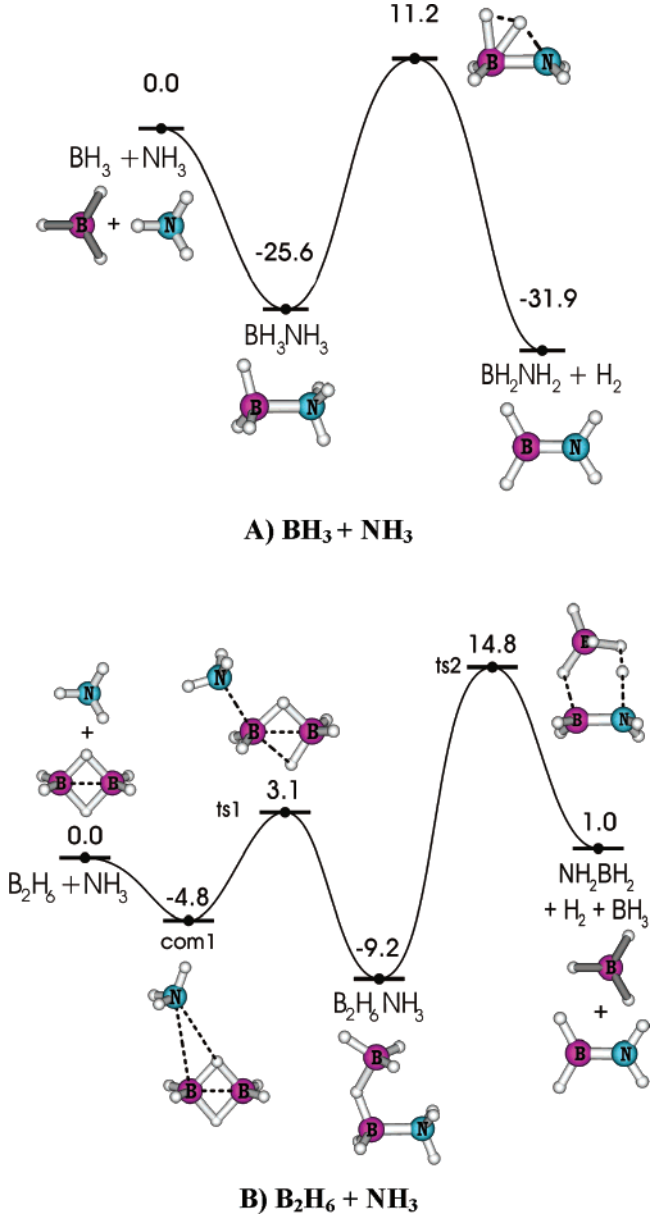

Figure 5. Reaction pathway for H_2 release at 0 K from (A) BH_3 + NH_3 and (B) B_2H_6 + NH_3. Relative energies, in kcal/mol, were obtained from CCSD(T)/aVTZ + ZPE calculations. For A, see ref 8 for the figure with the CCSD(T)/CBS + correction results.

properties of the adduct $B_2H_6NH_3$ and **ts2** for H_2 release have been analyzed in detail.[8] We note that **ts2** lies 11.7 kcal/mol above **ts1**; therefore, **ts2** is clearly the rate-determining step leading to H_2 release.[38] Other aspects of the (B_2H_9N) potential energy surface will be discussed in a subsequent paper.[39]

Reaction Pathways for H_2 Release from $B_3H_7NH_3$ Starting from atb3. The adducts collectively labeled **atb3** lead to a number of reaction pathways for H_2 generation. We summarize the relevant transition states to point out the rich possibilities for H_2 elimination, although these may not be energetically important. Selected MP2/aVTZ geometrical parameters of the transition states are displayed in Figure 6, and the energy profiles are shown in Figures 7 and 8. The optimized geometries of the products are given in Figure S-2 of the Supporting Information.

For each of the isomers **atb3-c1**, **atb3-t1**, **atb3-c**, and **atb3-t** considered, two transition states were located and are distinguished by the position of the departing H_2. In general, one

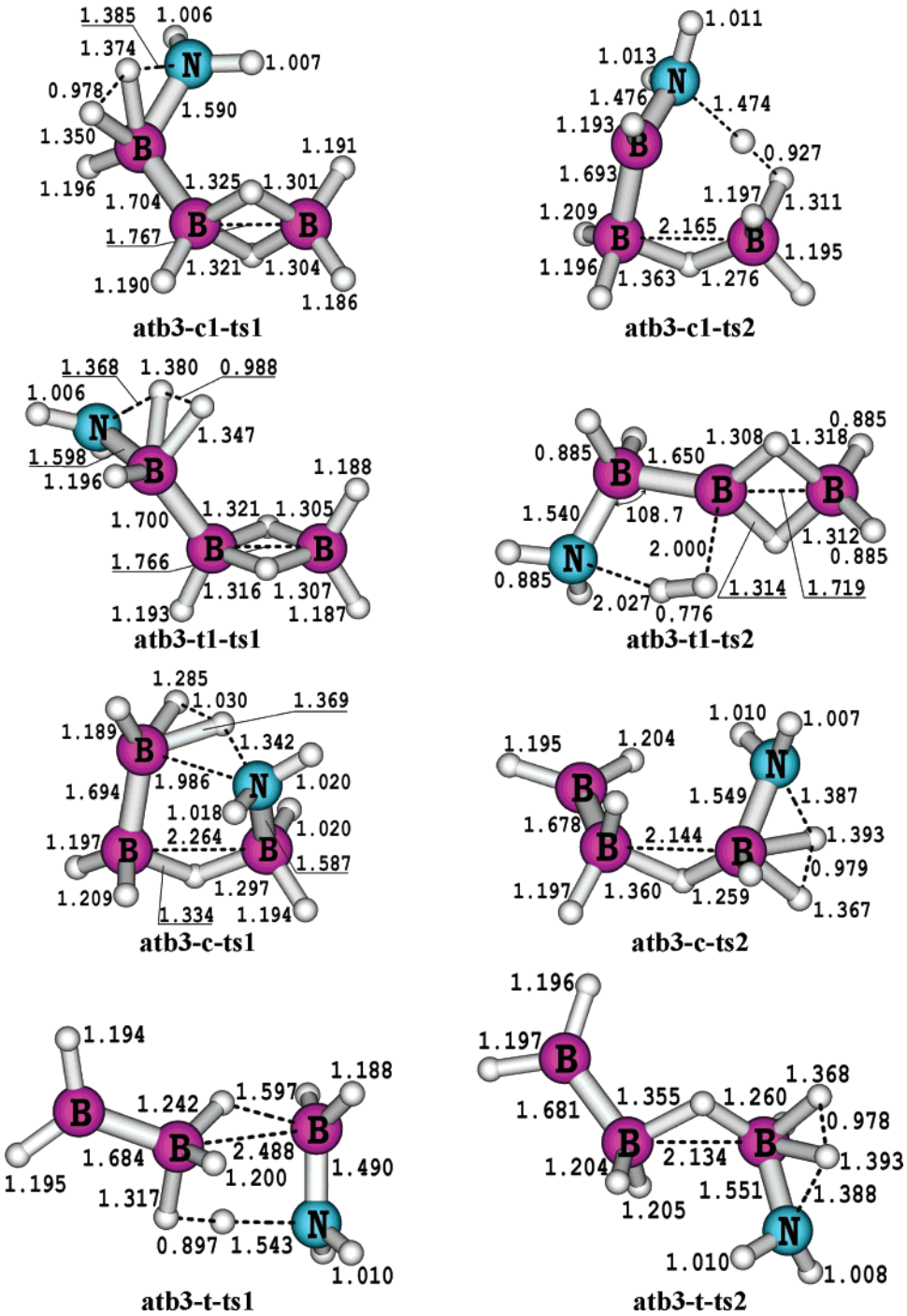

Figure 6. Selected MP2/aVTZ geometrical parameters of transition state structures for H_2 elimination of different adducts **atb3**. Bond distances are given in angstroms and bond angles in degree.

group of transition states closely resembles that of the parent BH_3NH_3 adduct and can be regarded as a 1,2-H_2-elimination with the remaining groups acting as a substituent. These include **atb3-c1-ts1**, **atb3-t1-ts1**, **atb3-c-ts2**, and **atb3-t-ts2**. The second group of transition states involves a H(B) from a boron nonbonded to the nitrogen and includes **atb3-c1-ts2**, **atb3-t1-ts2**, **atb3-c-ts1**, and **atb3-t-ts1**. A common characteristic of all the transition states for H_2 release is that they are higher in energy than the corresponding B−N dissociation energies. As a consequence, these processes are not expected to significantly contribute to the H_2 formation under mild thermal conditions.

As an example, we summarize the results regarding the energetically lowest-lying adduct formed from **atb3**. **atb3-c1** is associated with two different transition states in which the H_2 is produced from a H(N) atom and a hydrogen from one of the borons. These are denoted as **atb3-c1-ts1** and **atb3-c1-ts2** (Figure 6). **atb3-c1-ts1** is a 1,2-H_2-elimination process. In this case, 1,2-H_2-elimination has a lower energy barrier (Figure 7). A similar result is found for the **atb3-t1** isomer where 1,3-H_2-elimination proceeding through **atb3-t1-ts2** is of higher energy. The processes related to the less stable **atb3-c** and **atb3-t** are shown in Figure 8.

Kinetics of the Decomposition of Ammonia Triborane atb1. In contrast to BH_3NH_3 and $B_2H_6NH_3$, the energy barrier for 1,3-H_2-elimination of 28.9 kcal/mol through **atb1-ts1** is substantially lower than that for 1,2-H_2-elimination and is also slightly lower (by 1.8 kcal/mol) than the corresponding B−N

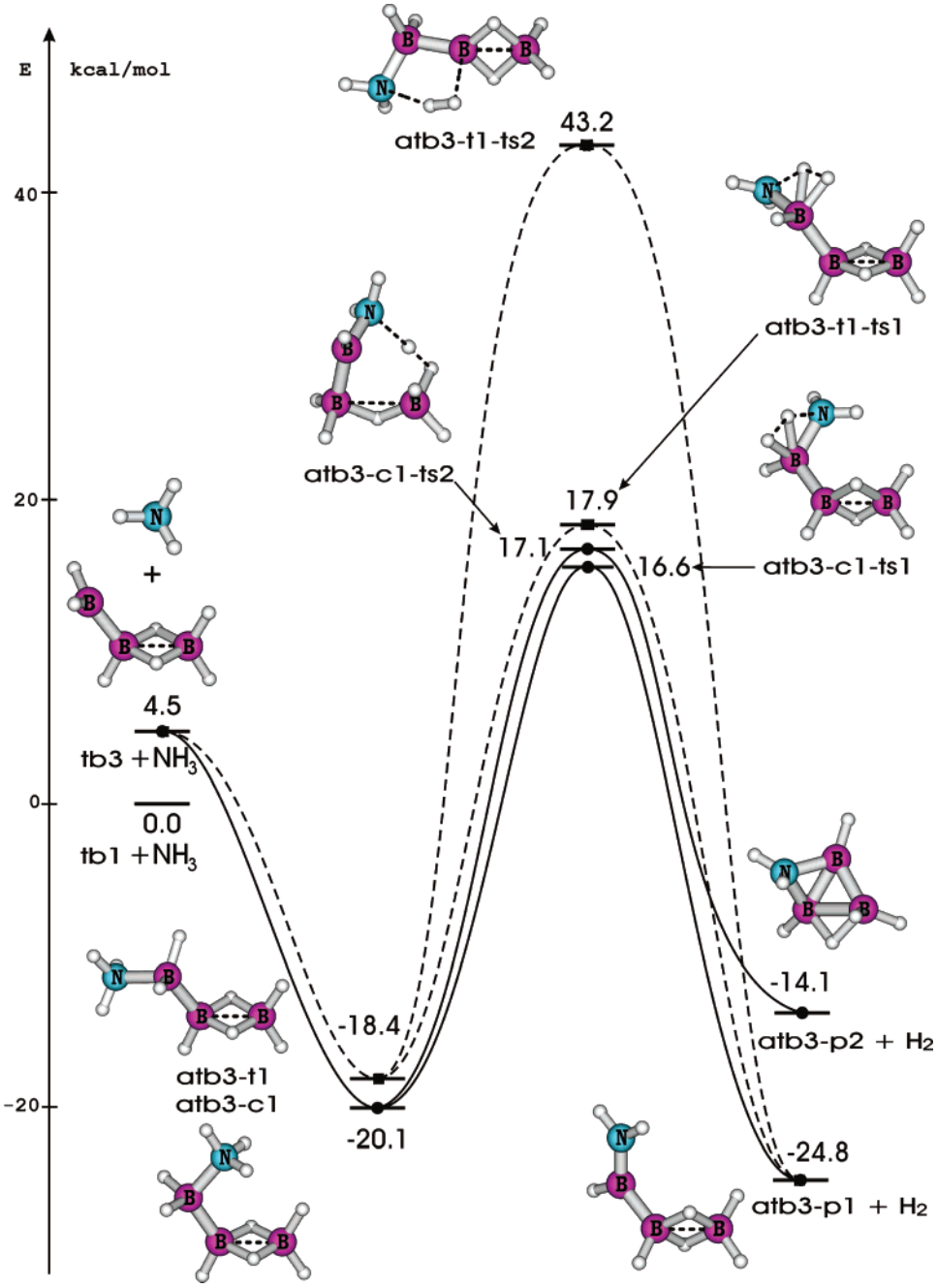

Figure 7. Schematic energy profiles illustrating different reaction pathways for H_2 release from **atb3-c1** and **atb3-t1**. Relative energies, in kcal/mol, were obtained from CCSD(T)/aVTZ + ZPE calculations at 0 K.

bond cleavage products. In view of the small energy difference, the outcome of the two competing unimolecular reactions requires estimates of the rate constants for each path. Whereas **atb1-ts1** is relatively compact, the formation of $B_3H_7 + NH_3$ is a simple bond dissociation process with no barrier and will have a larger effective entropy contribution leading to a faster rate for bond cleavage.

We performed a kinetic analysis considering both the B−N bond dissociation and H_2 loss channels using the RRKM theory for unimolecular reactions[40] with rate expression 4

$$k_{\text{uni}} = \frac{\sigma}{h}\left[\frac{N^{\ddagger}(E - E_0)}{\rho(E)}\right] \tag{4}$$

where σ is the symmetry number. Evaluation of the sum ($N^{\ddagger}$) and density (ρ) of states was carried out using the *KHIMERA* program.[41] The rate constant as a function of temperatures (T) and pressure (p) for the range of T from 200 to 1500 K and p from 0.1 to 8360 Torr is illustrated in 3-D representation in Figure 9. As in previous studies,[8] we treated the B−N dative bond-breaking reaction as a barrierless reaction. We used the MP2/aVTZ geometries and MP2/aVDZ vibrational frequencies combined with CCSD(T)/CBS total electronic energies. For this range of T(K) and p(Torr) with N_2 as the collision gas, the calculated rate constants can be fit to the general expressions (energy in kcal/mol)

$$k(T, p)_{\text{H}_2} = 1.26 \times 10^{11}\, p^{0.34} \exp\frac{-28.4}{RT} \tag{5}$$

$$k(T, p)_{\text{B-N}} = 7.94 \times 10^{11}\, p^{0.72} \exp\frac{-27.5}{RT} \tag{6}$$

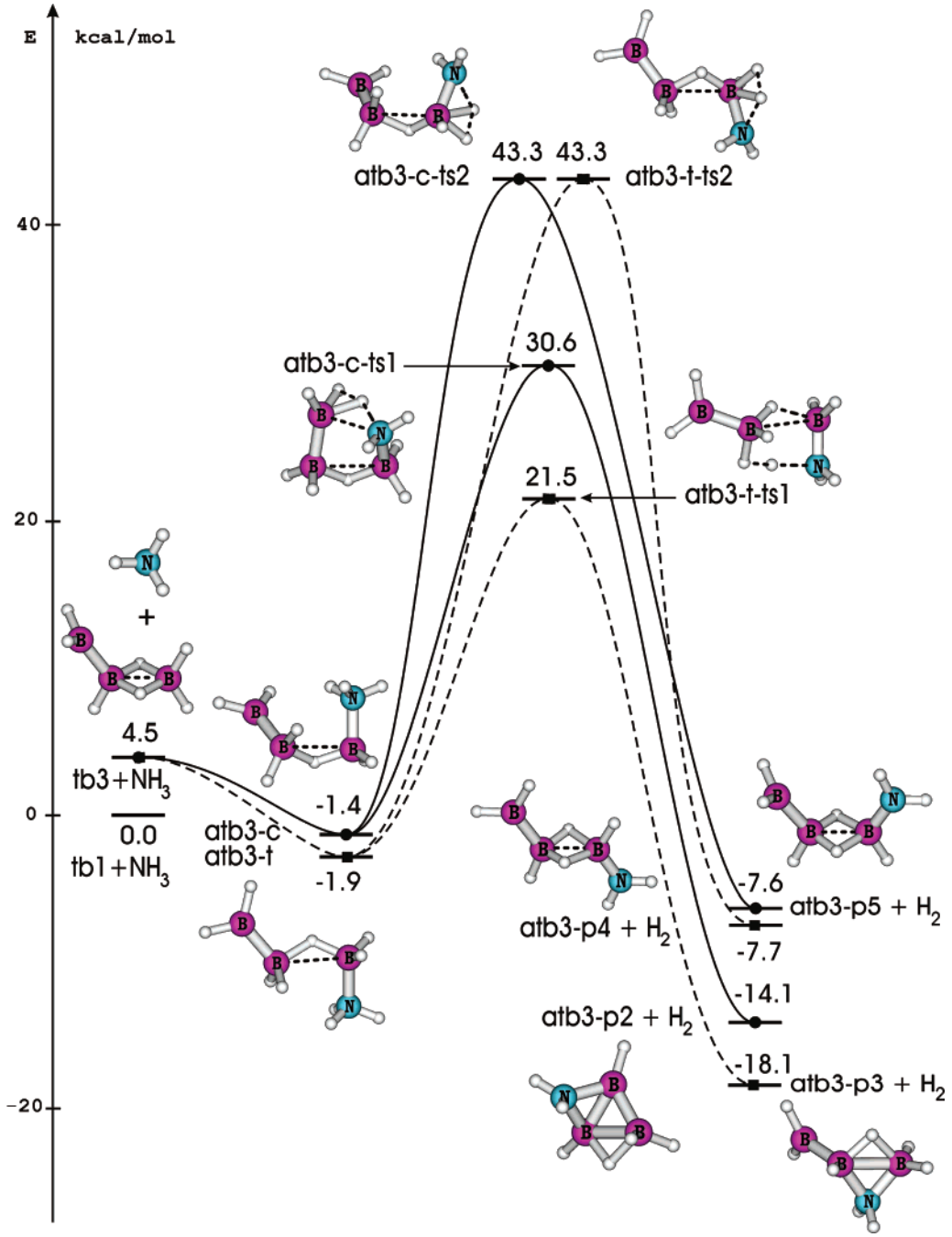

Figure 8. Schematic energy profiles illustrating different reaction pathways for H_2 release from **atb3-c** and **atb3-t**. Relative energies, in kcal/mol, were obtained from CCSD(T)/aVTZ + ZPE calculations at 0 K.

Calculations for the high-pressure thermal rates of the H_2 release channel were also carried out using the thermodynamic formulation (conventional transition state theory, TST).[41]

$$k(T)_{H_{2,TST}} = 3.98 \times 10^{10}\, T^{0.67} \exp\frac{-28.7}{RT} \qquad (7)$$

The rate coefficients obtained for H_2 loss are k_{H_2}(298 K, 1 atm) = 1.8×10^{-9} s^{-1} by TST and 2.0×10^{-9} s^{-1} by RRKM. Including a tunneling correction of Q_W(298 K) = 1.43 estimated using the Wigner equation,[42] the rate coefficients become k_{H_2}(298 K, 1 atm, Q_W) = 2.5×10^{-9} s^{-1} by TST and 2.9×10^{-9} s^{-1} by RRKM. Using the Skodje−Truhlar formula,[43] Q_{ST}(298 K) = 1.61, the following rates are obtained: k_{H_2}(298 K, 1 atm, Q_{ST}) = 2.9×10^{-9} s^{-1} by TST and 3.3×10^{-9} s^{-1} by RRKM (cf. refs 8 and 44 for more details of the kinetics calculations).

We can check the quality of our calculated value for the rate constant for breaking the B−N bond as follows. One can write $K = k_f/k_r$ where K is the equilibrium constant and k_f and k_r are the corresponding forward and reverse rate constants for reaction 8 (reverse process of reaction 3).

$$B_3H_7 + NH_3 \rightarrow B_3H_7NH_3 \qquad (8)$$

We obtain $K = 3.54 \times 10^{15}$ from our calculated values of ΔG = −21.2 kcal/mol. This value of ΔG is obtained from our calculated ΔH of −32.1 kcal/mol and from ΔS = −36.67 cal/mol−K at 298 K, using the experimental value[28] of $S(NH_3)$ = 46.07 cal/mol−K. By using our calculated value for k_r, the rate constant for bond dissociation ($k_{B-N} = 1.80 \times 10^{-6}$ s^{-1} at 298 K, 1 atm), we obtain a value of k_f (the recombination rate constant) of 1.06×10^{-11} cm^3/molecule−s. This value for k_f

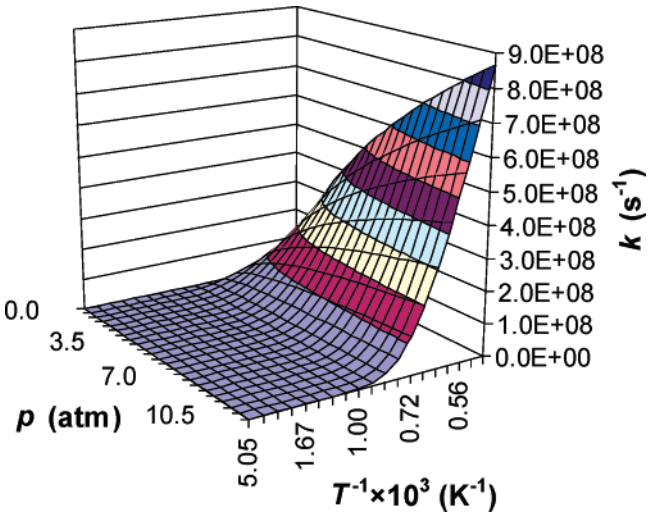

Figure 9. A 3-D plot of the rate coefficients k for the H_2 elimination from $B_3H_7NH_3$ calculated by using RRKM theory with N_2 as the bath gas in the temperature range (T) from 200 to 2000 K and bath gas pressure range (p) from 0.1 to 8360 Torr. Tunneling is not included.

can be compared to those obtained in radical recombination reactions, for example, $2CH_3 \rightarrow C_2H_6$ and other organic radical R· recombinations ($2R\cdot \rightarrow R-R$) which are on the order of 10^{-10} to 10^{-11} cm^3/molecule-s.[40,45] Our value is comparable to better than an order of magnitude with these results showing that our value for the dissociation process is reasonable.

At two different pressures, the decomposition thermal rate coefficients are $k_{B-N} = 1.80 \times 10^{-6}$ s^{-1} at 298 K, 1 atm, and $k_{B-N} = 1.84 \times 10^{-6}$ s^{-1} at 298 K, 11 atm. Similarly, the rate constants for H_2 elimination at 1 and 11 atm are nearly identical. These calculated rate coefficients clearly show that B−N bond cleavage of **atb1** is faster than H_2 loss by almost 3 orders of magnitude. The dominance of the B−N channel holds even at high temperatures (factor of 10^2 at 1000 K and 10 at 1500 K).

Concluding Remarks

Electronic structure calculations have been applied to calculate critical points on the potential energy surfaces related to hydrogen release from ammonia triborane $B_3H_7NH_3$. The molecular hydrogen release reaction is endothermic by 5.6 kcal/mol giving an aminotriborane ring. Starting from its most stable from in the gas phase, ammonia triborane can release one H_2 molecule by a direct 1,3-H_2-elimination pathway characterized by an energy barrier of 28.9 kcal/mol. 1,2-H_2-elimination is found to be a less favored process. In contrast to the parent homologues BH_3NH_3 and $B_2H_6NH_3$, the barrier height for H_2 release from $B_3H_7NH_3$ is slightly smaller than the B−N bond cleavage energy of 30.7 kcal/mol yielding the fragments $B_3H_7 + NH_3$. The thermal rate for the B−N bond scission is higher than that for the H_2 release, by up to a factor of 10^3 under the conditions of 298 K and 1 atm. These results show that a catalyst will be needed to develop adequate reaction conditions for H_2 release.

Acknowledgment. Funding provided in part by the Department of Energy, Office of Energy Efficiency and Renewable Energy under the Hydrogen Storage Grand Challenge, Solicitation No. DE-PS36-03GO93013. This work was done as part of the Chemical Hydrogen Storage Center. David A. Dixon is indebted to the Robert Ramsay Endowment of the University of Alabama. V.S.N. thanks the Belgian Technical Cooperation Agency (BTC) for a doctoral scholarship. M.T.N. is indebted to the FWO-Vlaanderen for supporting his sabbatical leave at the University of Alabama. We thank Dr. S. J. Klippenstein for helpful comments on the rates of unimolecular processes.

Supporting Information Available: Optimized geometries (Cartesian coordinates) at both MP2/aug-cc-pVDZ and MP2/aug-cc-pVTZ levels, CCSD(T) total energies, zero-point energies, harmonic vibrational frequencies and IR intensities of the B_3H_7 isomers, the $NH_3B_3H_7$ isomers, the transition structures for, and the products of H_2 release. Figures S-1 and S-2 show the selected MP2/aug-cc-pVTZ geometrical parameters of the products of H_2 elimination from **atb1** and different adducts **atb3**. This material is available free of charge via the Internet at http://pubs.acs.org.

References and Notes

(1) (a) *Basic Energy Needs for the Hydrogen Economy*; Dressalhaus, M., Crabtree, G., Buchanan, M., Eds.; Basic Energy Sciences, Office of Science, U. S. Department of Energy; U. S. Government Printing Office: Washington, DC, 2003. (b) Maelund, A. J.; Hauback, B. C. In *Advanced Materials for the Energy Conversion II*; Chandra, D., Bautista, R. G., Schlapbach, L., Eds.; The Minerals, Metals and Materials Society: Warrendale, PA, 2004.

(2) Parry, R. W.; Schultz, D. R.; Girardot, P. R. *J. Am. Chem. Soc.* **1958**, *80*, 1.

(3) Sorokin, V. P.; Vesnina, B. I.; Klimova, N. S. *Russ. J. Inorg. Chem.* **1963**, *8*, 32.

(4) (a) Geanangel, R. A.; Wendlandt, W. W. *Thermochim. Acta* **1985**, *86*, 375. (b) Sit, V.; Geanangel, R. A.; Wendlandt, W. W. *Thermochim. Acta* **1987**, *113*, 379. (c) Wang, J. S.; Geanangel, R. A. *Inorg. Chim. Acta* **1988**, *148*, 185.

(5) (a) Wolf, G.; van Miltenburg, R. A.; Wolf, U. *Thermochim. Acta* **1998**, *317*, 111. (b) Wolf, G.; Baumann, J.; Baitalow, F.; Hoffmann, F. P. *Thermochim. Acta* **2000**, *343*, 19. (c) Baitalow, F.; Baumann, J.; Wolf, G.; Jaenicke-Rlobler, K.; Leitner, G. *Thermochim. Acta* **2002**, *391*, 159.

(6) Dixon, D. A.; Gutowski, M. *J. Phys. Chem. A* **2005**, *109*, 5129.

(7) Grant, D.; Dixon, D. A. *J. Phys. Chem. A* **2005**, *109*, 10138.

(8) Nguyen, M. T.; Nguyen, V. S.; Matus, M. H.; Gopakumar, G.; Dixon, D. A. *J. Phys. Chem. A* **2007**, *111*, 679.

(9) Yoon, C. W.; Sneddon, L. G. *J. Am. Chem. Soc.* **2006**, *128*, 13992.

(10) (a) Nordman, C. E. *Acta Crystallogr.* **1957**, *10*, 777. (b) Nordman, C. E.; Reiman, C. *J. Am. Chem. Soc.* **1959**, *81*, 3538.

(11) Kodama, G.; Parry, R. W.; Carter, J. C. *J. Am. Chem. Soc.* **1959**, *81*, 3534.

(12) Westrum, E. F.; Levitin, N. E. *J. Am. Chem. Soc.* **1959**, *81*, 3544.

(13) Frisch, M. J.; Trucks, G. W.; Schlegel, H. B.; Scuseria, G. E.; Robb, M. A.; Cheeseman, J. R.; Montgomery, J. A., Jr.; Vreven, T.; Kudin, K. N.; Burant, J. C.; Millam, J. M.; Iyengar, S. S.; Tomasi, J.; Barone, V.; Mennucci, B.; Cossi, M.; Scalmani, G.; Rega, N.; Petersson, G. A.; Nakatsuji, H.; Hada, M.; Ehara, M.; Toyota, K.; Fukuda, R.; Hasegawa, J.; Ishida, M.; Nakajima, T.; Honda, Y.; Kitao, O.; Nakai, H.; Klene, M.; Li, X.; Knox, J. E.; Hratchian, H. P.; Cross, J. B.; Bakken, V.; Adamo, C.; Jaramillo, J.; Gomperts, R.; Stratmann, R. E.; Yazyev, O.; Austin, A. J.; Cammi, R.; Pomelli, C.; Ochterski, J. W.; Ayala, P. Y.; Morokuma, K.; Voth, G. A.; Salvador, P.; Dannenberg, J. J.; Zakrzewski, V. G.; Dapprich, S.; Daniels, A. D.; Strain, M. C.; Farkas, O.; Malick, D. K.; Rabuck, A. D.; Raghavachari, K.; Foresman, J. B.; Ortiz, J. V.; Cui, Q.; Baboul, A. G.; Clifford, S.; Cioslowski, J.; Stefanov, B. B.; Liu, G.; Liashenko, A.; Piskorz, P.; Komaromi, I.; Martin, R. L.; Fox, D. J.; Keith, T.; Al-Laham, M. A.; Peng, C. Y.; Nanayakkara, A.; Challacombe, M.; Gill, P. M. W.; Johnson, B.; Chen, W.; Wong, M. W.; Gonzalez, C.; Pople, J. A. *Gaussian 03*, revision C.01; Gaussian, Inc.: Wallingford, CT, 2004.

(14) Amos, R. D.; Bernhardsson, A.; Berning, A.; Celani, P.; Cooper, D. L.; Deegan, M. J. O.; Dobbyn, A. J.; Eckert, F.; Hampel, C.; Hetzer, G.; Knowles, P. J.; Korona, T.; Lindh, R.; Lloyd, A. W.; McNicholas, S. J.; Manby, F. R.; Meyer, W.; Mura, M. E.; Nicklass, A.; Palmieri, P.; Pitzer, R.; Rauhut, G., Schütz, M.; Schumann, U.; Stoll, H., Stone, A. J.; Tarroni, R.; Thorsteinsson, T.; Werner, H.-J. *MOLPRO* a package of *ab initio* programs designed by Werner, H.-J., and Knowles, P. J., version 2002.6.

(15) Pople, J. A.; Seeger, R.; Krishnan, R. *Int. J. Quantum Chem. Chem. Symp.* **1977**, *11*, 149.

(16) (a) Dunning, T. H., Jr. *J. Chem. Phys.* **1989**, *90*, 1007. (b) Kendall, R. A.; Dunning, T. H., Jr.; Harrison, R. J. *J. Chem. Phys.* **1992**, *96*, 6796.

(17) Gonzalez, C.; Schlegel, H. B. *J. Chem. Phys.* **1989**, *90*, 2154.

(18) (a) Cizek, J. *Adv. Chem. Phys.* **1969**, *14*, 35. (b) Purvis, G. D.; Bartlett, R. J. *J. Chem. Phys.* **1982**, *76*, 1910. (c) Pople, J. A.; Head-Gordon, M.; Raghavachari, K. *J. Chem. Phys.* **1987**, *87*, 5968.

(19) Feller; D.; Dixon, D. A.; Peterson, K. A. *J. Phys. Chem. A* **1998**, *102*, 7053.

(20) Shimanouchi, T. *Tables of Molecular Vibration Frequencies Consolidated, Vol. I*; NSRDS-NBS 39; NBS, U. S. Government Printing Office: Washington, DC, 1972.

(21) Peterson, K. A.; Woon, D. E.; Dunning, T. H., Jr. *J. Chem. Phys.* **1994**, *100*, 7410.

(22) (a) Peterson, K. A.; Dunning, T. H., Jr. *J. Chem. Phys.* **2002**, *117*, 10548. (b) Woon, D. E.; Dunning, T. H., Jr. *J. Chem. Phys.* **1993**, *98*, 1358.

(23) Davidson, E. R.; Ishikawa, Y.; Malli, G. L. *Chem. Phys. Lett.* **1981**, *84*, 226.

(24) Moore, C. E. *Atomic energy levels as derived from the analysis of optical spectra*; U.S. National Bureau of Standards Circular 467; U.S. Department of Commerce; National Technical Information Service; COM-72-50282; U. S. Government Printing Office: Washington, DC, 1949; Vol. 1, H to V.

(25) Rittby, M.; Bartlett, R. J. *J. Phys. Chem*. **1988**, *92*, 3033.

(26) Knowles, P. J.; Hampel, C.; Werner, H.-J. *J. Chem. Phys*. **1994**, *99*, 5219.

(27) Deegan, M. J. O.; Knowles, P. J. *Chem. Phys. Lett.* **1994**, *227*, 321.

(28) Chase, M. W., Jr. NIST-JANAF Tables (4th Edition). *J. Phys. Chem. Ref. Data* **1998**, Mono. 9, Suppl. 1. See also Linstrom, P. J., Mallard, W. G., Eds. *NIST Chemistry WebBook*, NIST Standard Reference Database Number 69, June 2005, National Institute of Standards and Technology, Gaithersburg MD, 20899 (http://webbook.nist.gov/chemistry/).

(29) (a) Ruscic, B.; Mayhew, C. A.; Berkowitz, J. *J. Chem. Phys*. **1988**, *88*, 5580. (b) Storms, E.; Mueller, B. *J. Phys. Chem*. **1977**, *81*, 318; Ochterski, J. W.; Petersson, G. A.; Wiberg, K. B. *J. Am. Chem. Soc.* **1995**, *117*, 11299.

(30) Curtiss, L. A.; Raghavachari, K.; Redfern, P. C.; Pople, J. A. *J. Chem. Phys.* **1997**, *106*, 1063.

(31) (a) Ortiz, J. V.; Lipscomb, W. N. *Chem. Phys. Lett.* **1983**, *103*, 59. (b) Mckee, M. L.; Lipscomb, W. N. *Inorg. Chem.* **1982**, *21*, 2846. (c) McKee, M. L. *J. Phys. Chem.* **1990**, *94*, 435.

(32) Cheng, M. F.; Ho, H. O.; Lam, C. S.; Li, W. K. *Chem. Phys. Lett.* **2002**, *356*, 109.

(33) Tian, S. X. *J. Phys. Chem. A* **2005**, *109*, 5471.

(34) McKee, M. L. *Inorg. Chem.* **1988**, *27*, 4241.

(35) Feller, D.; Dixon, D. A.; Peterson, K. A. *J. Phys. Chem. A* **1998**, *102*, 7053.

(36) (a) Klooster, W. T.; Koetzle, T. F.; Siegbahn, P. E. M.; Richardson, T. B.; Crabtree, R. H. *J. Amer. Chem. Soc.* **1999**, *121*, 6337. (b) Popelier, P. L. A. *J. Phys. Chem. A* **1998**, *102*, 1873.

(37) (a) Trudel, S.; Gilson, D. F. R. *Inorg. Chem.* **2003**, *42*, 2814. (b) Morrison, C. A.; Siddick, M. M. *Angew. Chem., Int. Ed.* **2004**, *116*, 4884.

(38) (a) Sakai, S. *Chem. Phys. Lett.* **1994**, *217*, 288. (b) Sakai, S. *J. Phys. Chem.* **1995**, *99*, 9080.

(39) Nguyen, V. S.; Matus, M. H.; Nguyen, M. T.; Dixon, D. A. Unpublished data, 2007.

(40) Holbrook, K. A.; Pilling, M. J.; Robertson, S. H. *Unimolecular Reactions*, 2nd ed.; Wiley: Chichester, U.K., 1996.

(41) *KHIMERA*, v 3.2: A software tool for calculations of chemical reactions thermodynamics and kinetics from first principles; Kintech, Kinetic Technologies, Ltd., Moscow, 2003. http://www.kintech.ru/.

(42) Wigner, E. Z. *Z. Phys. Chem. B* **1932**, *19*, 203.

(43) Skodje, R. T.; Truhlar, D. J. *J. Chem. Phys.* **1981**, *85*, 624.

(44) Matus, M. H.; Nguyen, M. T.; Dixon, D. A. *J. Phys. Chem. A* **2007**, *111*, 113.

(45) Klippenstein, S. J.; Harding, L. B. *J. Phys. Chem. A* **1999**, *103*, 9388. Klippenstein, S. J.; Georgievskii, Y.; Harding, L. B. *Phys. Chem. Chem. Phys.* **2006**, *8*, 1133.